Modeling of self-piercing riveted joints for crash simulation – state of the art and future topics

Matthias Bier[1], Silke Sommer[1]

[1] Fraunhofer Institute for Mechanics of Materials IWM, Freiburg, Germany

1 Abstract

The requirements for energy efficiency and lightweight construction in automotive engineering rise steadily. Therefore a maximum flexibility of different materials is necessary and new joining techniques are constantly developed. The resulting large number of joints with different properties leads to the need to provide for each type of joint an appropriate modeling method for crash simulation.

In recent years the ***CONSTRAINED_INTERPOLATION_SPOTWELD** was modified to improve the modeling of the behavior of self-piercing riveted joints. The modified version will be available in LS-Dyna soon. This paper gives a short overview about the background and shows the benefits and limitations of the model. Furthermore, future research topics are shown for increasing the model quality. Topics like the influence of deformations in the surrounding sheets and the local loading situation on the rivet behavior will be discussed. For this purpose simulation results of variations of the lap shear specimen are shown and compared with experimental data.
First results of a German research project called “Characterization and modeling of mechanical joints with one-sided accessibility for profile intensive lightweight construction under crash loading” will be presented.
The Industrial Collective Research project (IGF-Nr. 18289 N / FOSTA P1032) of the Research Association for Steel Application (FOSTA), Sohnstrasse 65, 40237 Duesseldorf has been funded by the German Federation of Industrial Research Associations „Otto von Guericke“ e.V. (AiF) within the program for sponsorship of Industrial Collective Research (IGF) of the German Federal Ministry of Economic Affairs and Energy (BMWi) based on an enactment of the German Bundestag.

2 Introduction

In this paper self-piercing riveting, more precisely self-piercing riveting with a semi-tubular rivet, is examined. Self-piercing riveting (SPR) belongs to the group of mechanical joining techniques to join two or more sheets.

The processes can be divided into four different steps as it is described by He et al. [1] (see Fig. 1). The first step is the clamping. Thereby the blank holder and the die compress the assembly parts, which will be joined. Thus the relative position of the two or more sheets is fixed and the rivet is put onto the sheets. The second step is the piercing. This is the first step, where deformations occur. The punch drives the rivet through the top sheet metal into the bottom sheet metal. In doing so, the rivet punches a hole into the top sheet and the punched-out top sheet material flows inside the rivet. The third step is the flaring. The die in combination with the material inside the rivet deform the rivet, thus an interlock is formed. The last step is the releasing. In this step, the punch stops pushing the rivet and the blank holder releases the joined sheets. The riveting process is finished.

The advantage of SPR is the possibility to join a range of dissimilar materials. The only requirement to the joined materials is an appropriate ductility, so that the joint can be formed appropriately. Furthermore the joining process of self-piercing rivets does not affect the microstructure and thus the properties of the joined materials, as it can be observed in thermal joining processes.
These advantages are the reasons, why SPR is increasingly used in lightweight construction of automotive engineering, especially in case of joints between two sheets of aluminum or aluminum and steel.

© 2015 Copyright by DYNAmore GmbH

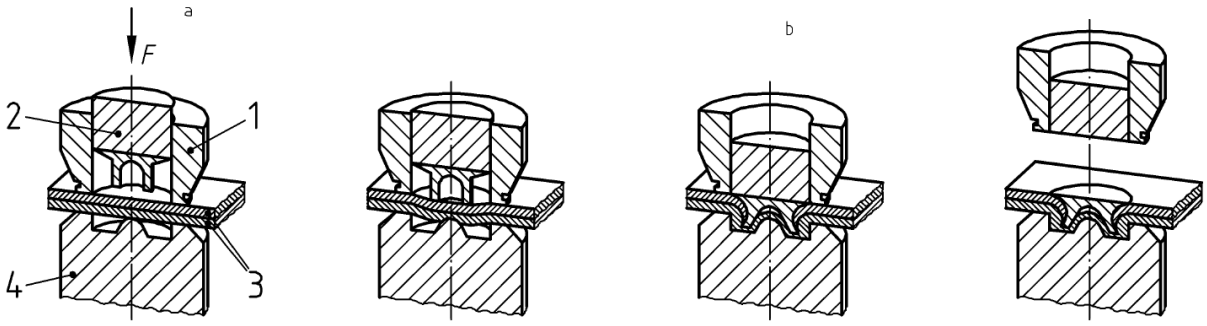

Fig.1: Joining process of a self-piercing rivet connection, schematic representation (1 – blank holder, 2 – punch, 3 – assembly parts, 4 – female die) [2]

Currently in full vehicle simulations different simplified models are used for punctiform joints. Seeger et al. [3] presented a new failure criterion for a model based on von Mises plasticity. This is known in LS-Dyna as ***MAT_100_DA** and is now frequently used as a model for spot welds in full vehicle simulations. Bier et al. [4] compared the ***MAT_100_DA** with the ***MAT_COHESIVE_MIXED_MODE_ELASTOPLASTIC_RATE (*MAT_240**), developed by Marzi et al. [5] for adhesively bonded joints, with respect to the usage of spot weld modeling and mesh sensitivity. Hanssen et al. [6] developed a model for self-piercing rivet connections, which is implemented in LS-Dyna as ***Constrained_SPR2**. The ***Constrained_SPR2** considers the relative motion of the connected sheets and calculates the transferred forces and moments from these motions. Another model used for punctiform joints is the ***Constrained_SPR3** [7], also named ***Constrained_Interpolation_Spotweld**, which is based on the ***Constrained_SPR2** with a different flow and damage behavior. Sommer et al. [8] investigated all these models and in addition the ***MAT_169** [7] with respect to modeling possibilities of self-piercing rivet connections. They identified in all models different weaknesses. Buckley et al. [10] presented a material model for self-piercing rivet joints (***MAT_SPR_JLR**), which is based on investigations on detailed models [11] and represents the joint by the behavior of a combination of spring and beam elements.
Bier et al. developed [9] and presented [12] a modified version of the ***Constrained_SPR3** for self-piercing rivet joints, which will be implemented in LS-Dyna as the Model 2 option of the ***Constrained_SPR3** and is used for the following investigations.

3 Description of the simplified Model *Constrained_SPR3 (Model 2)

The ***Constrained_SPR3 (Model 2)** is based on the calculation of the relative motions of the connected sheets.
By definition of a reference node N_{ref}, which locates the position of the fastener, and a related radius r of the domain of influence the nodes of the connected sheets are determined, which are used to represent the connection. These nodes can be used to calculate the unit vectors $\vec{n}_m$and $\vec{n}_s$, which are orthogonal to the master and the slave sheet, respectively. By averaging the normal vectors of both sheets

$$\vec{n}_n = \frac{\vec{n}_m + \vec{n}_s}{|\vec{n}_m + \vec{n}_s|} \tag{1}$$

the direction of normal loads and by the equation

$$\vec{n}_t = (\vec{n}_s \times \vec{n}_m) \times \vec{n}_m \tag{2}$$

the shear direction can be identified. The total relative displacement $\vec{\delta}$ can be divided into two parts, one part δ_n in direction of $\vec{n}_n$

$$\delta_n = \vec{\delta} \cdot \vec{n}_n \tag{3}$$

and the second part δ_t in direction $\vec{n}_t$

$$\delta_t = \vec{\delta} \cdot \vec{n}_t. \tag{4}$$

© 2015 Copyright by DYNAmore GmbH

This vector of the relative motion can be used to get the transferred forces and moments and to describe the flow and failure behavior and is calculated by

$$\vec{u} = [\delta_n, \delta_t]. \tag{5}$$

In addition sym, which is an indicator for the symmetry of the rivet load [9], is calculated by

$$sym = \arccos \frac{\vec{n}_s \cdot \vec{n}_m}{|\vec{n}_s||\vec{n}_m|}. \tag{6}$$

Considering the joint stiffness $STIFF$ the transferred forces can be determined by

$$\begin{aligned} \vec{f} &= [f_n, f_t] \\ &= STIFF \cdot \vec{u} \\ &= STIFF \cdot [\delta_n, \delta_t]. \end{aligned} \tag{7}$$

Associated plastic flow with the yield surface

$$\left[\left(\frac{f_n}{R_n \cdot (1 - \alpha_1 \cdot sym)}\right)^{\beta_1} + \left(\frac{f_s}{R_s}\right)^{\beta_1}\right]^{\frac{1}{\beta_1}} - F^0(\bar{u}^{pl}) = 0 \tag{8}$$

is implemented. Linear scaling of the transferred forces

$$\vec{f}^* = (1 - d)\vec{f} \tag{9}$$

with the damage value

$$d = \frac{\bar{u}^{pl} - \bar{u}_0^{pl}}{\bar{u}_f^{pl} - \bar{u}_0^{pl}} \tag{10}$$

is done. For this purpose $\bar{u}_f^{pl}$ and $\bar{u}_0^{pl}$ are calculated considering the load angle φ

$$\varphi = \arctan\left(\frac{f_n}{f_s}\right) \tag{11}$$

and the following equations

$$\left[\left(\frac{\bar{u}_0^{pl,n}}{\bar{u}_{0,ref}^{pl,n} \cdot (1 - \alpha_2 * sym)}\right)^{\beta_2} + \left(\frac{\bar{u}_0^{pl,s}}{\bar{u}_{0,ref}^{pl,s}}\right)^{\beta_2}\right]^{\frac{1}{\beta_2}} - 1 = 0 \tag{12}$$

$$\bar{u}_0^{pl,n} = \sin(\varphi) \cdot \bar{u}_0^{pl} \tag{13}$$

$$\bar{u}_0^{pl,s} = cos(\varphi) \cdot \bar{u}_0^{pl} \tag{14}$$

$$\left[\left(\frac{\bar{u}_f^{pl,n}}{\bar{u}_{f,ref}^{pl,n} \cdot (1 - \alpha_3 * sym)}\right)^{\beta_3} + \left(\frac{\bar{u}_f^{pl,s}}{\bar{u}_{f,ref}^{pl,s}}\right)^{\beta_3}\right]^{\frac{1}{\beta_3}} - 1 = 0 \tag{15}$$

$$\bar{u}_f^{pl,n} = \sin(\varphi) \cdot \bar{u}_f^{pl} \tag{16}$$

$$\bar{u}_f^{pl,s} = cos(\varphi) \cdot \bar{u}_f^{pl}. \tag{17}$$

© 2015 Copyright by DYNAmore GmbH

4 Parameter determination/identification

The Parameter identification can be done in the following seven steps.

Step 1: *Domain of influence*

In the first step the radius of the domain of influence must be defined. This value should be equal or in the order of the rivet head radius.

Step 2: *Stiffness*

The stiffness $STIFF$ of the joint can be determined by the force vs. displacement curve of a shear test of the joint like KS-2-0° or a lap shear test. Based on the small deformations of the sheets $STIFF$ can be estimated in the linear area by

$$STIFF = \frac{\Delta F}{\Delta s} \tag{18}$$

Thereby ΔF and Δs are the force and displacement differences in the approximately linear area of the force vs. displacement curve, in which the stiffness will be averaged.

Step 3: *Shape of the flow curve*

Also the flow curve can be determined using the results of shear specimen tests. As for the determination of the stiffness, the approach is based on the assumption that the deformations of the sheets are small and only local deformations occur. These small and local deformations cannot be described by discretization usually used in crash simulation. So these are all included in the plastic deformations of the simplified model.

$$u_{pl} = \left(s - \frac{F(s)}{STIFF}\right) R_s \tag{19}$$

Step 4: *Maximum Forces*

The maximum transferred forces by the ***Constrained_SPR3 (Model 2)** represented by the parameters R_n and R_s are equal to the maximum measured forces in case of a normal and shear specimen test, respectively.

Step 5: *Combination of shear and tensile load*

The behavior in case of combined shear and tensile load is determined using KS-2-30° or 60° test results. Also it is possible to use another test with a combined shear and tensile load. Solving the equation

$$\left(\frac{f_n}{R_n}\right)^{\beta_1} + \left(\frac{f_s}{R_s}\right)^{\beta_1} = 1 \tag{20}$$

with the maximum force split in the normal and shear fraction by

$$f_n = sin\varphi \cdot F_{max}^{\varphi} \tag{21}$$

$$f_s = cos\varphi \cdot F_{max}^{\varphi} \tag{22}$$

leads to the value of β_1.

Step 6: *Damage and Failure behavior*

The determination of the parameters for the damage and failure behavior should be done by reverse engineering.

Step 7: *Influence of sym*

Also the weighting coefficients $\alpha_1, \alpha_2, \alpha_3$ should be determined by reverse engineering using peeling test results.

5 Simulation results and interpretations

The simulation results of the KS-2 specimens with ***Constrained_SPR3 (Model 2)** in comparison with test data [13] is shown in Fig.2. The simulation matches both, the transferred force and failure displacement, in all load cases. This leads to the conclusion, that the ***Constrained_SPR3 (Model 2)** is appropriate as a simplified model for self-piercing riveted joints.

© 2015 Copyright by DYNAmore GmbH

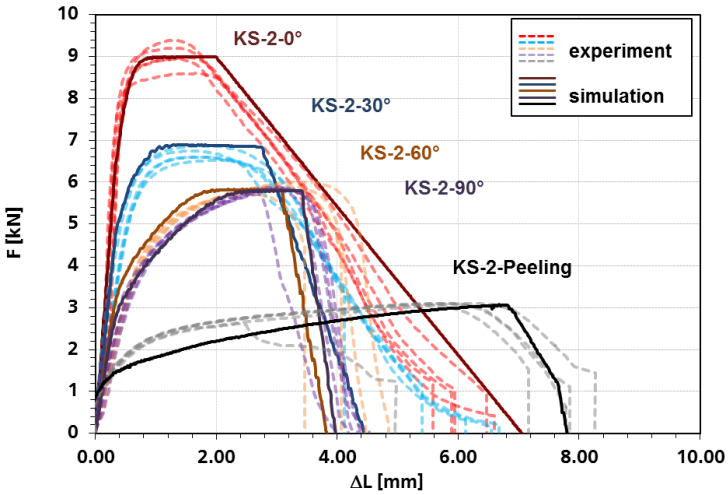

Fig.2: Simulation results of quasi-static KS-2-0°, 30°, 60°, 90° and peeling test with the modified ****Constrained_SPR3 (Model 2)*** *in comparison with experimental data [13].*

To validate the model, in [13] experimental investigations of riveted specimens called T-joints were done by the Laboratorium für Werkstoff- und Fügetechnik LWF in Paderborn. The geometry of the T-joint and the loading direction is shown in Fig.3. Exact dimensions and description of the simulation model can be found in [13]. The T-joint is modeled in LS-Dyna using the **`*Constrained_SPR3 (Model 2)`** with the parameters above for all nine SPR-joints.

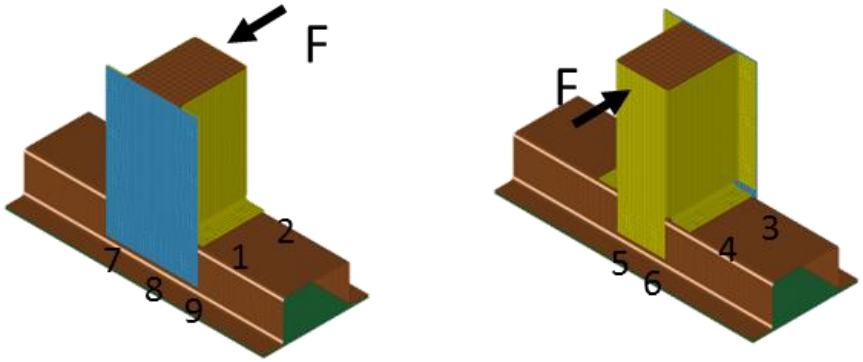

Fig.3: T joint geometry and loading direction (F); positon and numbering of the relevant self-piercing riveted joints(1-9)

The result of the simulation is shown in Fig. 4a) in comparison with the experimental data. An overestimation of the first maximum of the punch force can be observed. To understand the reason for the discrepancy the local loading situation is analyzed (see Fig. 4b)). The first maximum is dominated by the behavior of the rivets number 5 and 6, which are loaded almost in pure shear direction.

© 2015 Copyright by DYNAmore GmbH

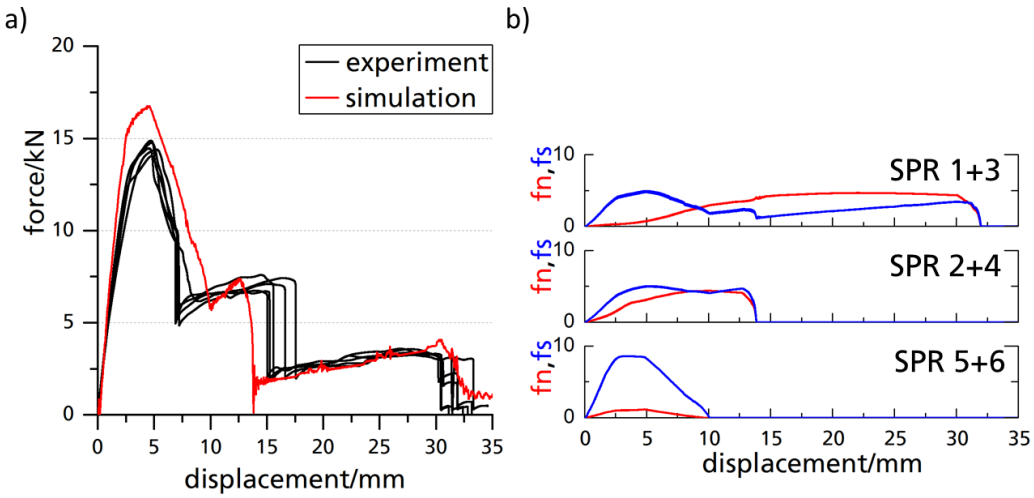

Fig.4: a) Global force vs. displacement curve as a result of the simulation of quasi-static T-joint tests (red) compared with experimental data [13]; b) local loading situation of the relevant ****Constrained_SPR3*** *during the quasi-static T-joint simulation (shear force fs – blue, normal force fn – red)*

The stiffness of the sheets in the area of the rivets 5 and 6 is lower than in case of the KS-2-0° load. Deformations can occur and lead to a change in the local loading situation. This loading situation is much more similar to the loading situation in the lap shear specimen [14], which is not used for the model calibration. The simulation result for the lap shear specimen compared with experimental data is shown in Fig. 5. The simplified model overestimates the transferred forces. The reached maximum force is similar to the maximum force in case of KS-2-0° load. On the opposite in experiments a decrease of the maximum force by about 1.5kN or 16% from the KS-2-0° to the lap shear specimen can be observed. This decrease of the load capacity, which is caused by the lower stiffness of the sheets, the rotation of the rivet and the resulting different sheet deformations, cannot be captured by the **`*Constrained_SPR3 (Model 2)`**. However other simplified models will show the same results.

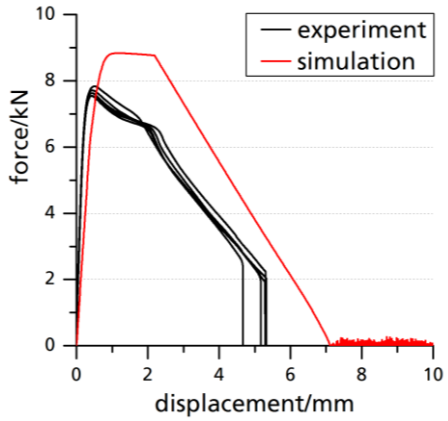

Fig.5: Simulation results (red) of quasi-static lap shear test with the ****Constrained_SPR3 (Model 2)*** *in comparison with experimental data (black) [13], KS-2-0° specimen used for parameter identification*

The reason is that all actual models represent the joint between undamaged sheets. In reality the sheets are damaged in the piercing step. The resulting hole, which is not included in the current simplified models and modelling of the sheets, affects the loading situation in the sheets. Fig. 6 shows simulation results of a lap shear specimen test. In the detailed model, the area of maximum load is on the pressure side, as caused by the hole in the sheet the rivet can just transfer pressure and no tension in shear direction. On the opposite the simplified model acts like an undamaged sheet and the simplified model leads to tensile load in the sheet elements.

© 2015 Copyright by DYNAmore GmbH

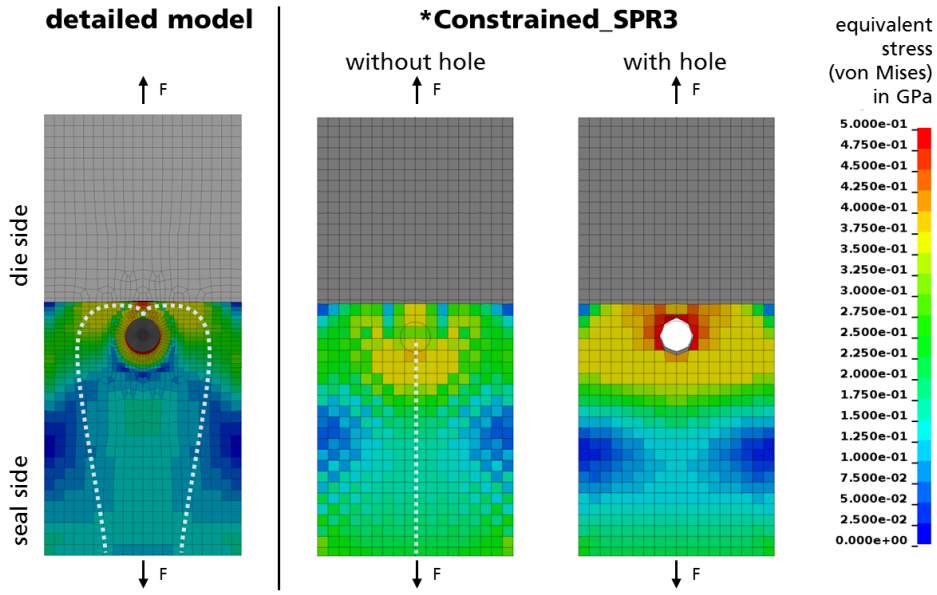

*Fig.6: Simulation results of lap shear specimen tests with equivalent stress (von Mises) as contour plot at the point of maximum force for three different modeling techniques (left to right: detailed model, ***Constrained_SPR3 (Model 2)** with undamaged sheets, ***Constrained_SPR3 (Model 2)** with hole in the connection area)*

In experiments and detailed simulations, the forces on the pressure side and weakening of the sheets by the hole lead to buckling on the free edge of the top sheet. In contrast the undamaged sheets in simulations with simplified models remain almost plane. Therefore the simplified models cannot detect the difference between the lap shear specimen and the KS-2-0° specimen, because in both cases the deformations of the shells are very similar.
One way to fix this problem is to use the lap shear specimen to identify the value of the parameter R_s. The results of simulations of the KS-2-0° specimen and the lap shear specimen with this changed value of R_s are shown in Fig. 7 a) and b). With this value it is possible to match the maximum force in case of the lap shear tests, but in case of the KS-2-0° simulation the maximum force is underestimated as much as the lap shear specimen is overestimated with the first set of parameters. The changed value of R_s also affects the result of the T-joint simulation (see Fig. 7 c)). The first force maximum, which is mainly influenced by R_s, matches now the measured value. Using the lap shear specimen to identify the value of the parameter R_s might be not the best option in all cases. If the flange geometry and properties are closer to the KS-2-0° specimen than to the lap shear specimen, the first set of parameters would be the better option.

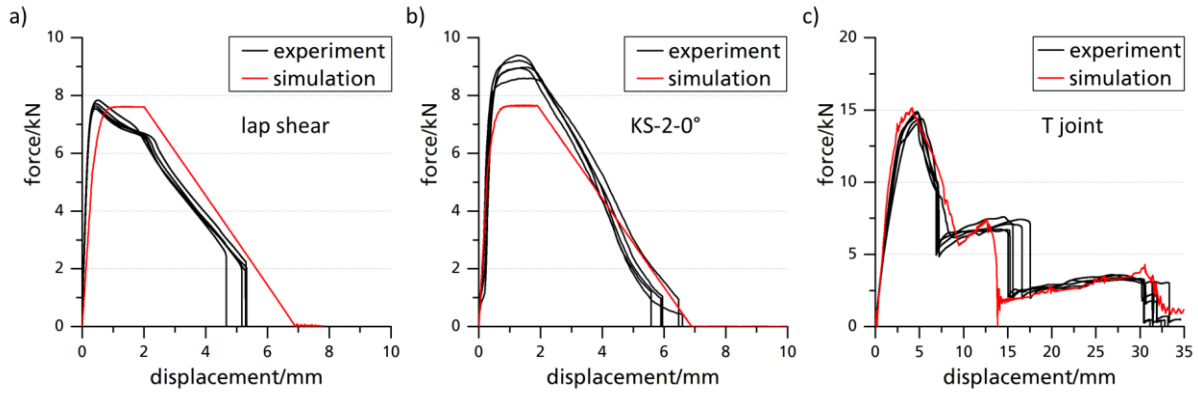

*Fig.7: Global force vs. displacement curves as a result of simulations with the ***Constrained_SPR3 (Model 2)** (red) - lap shear specimen used for model parameter identification - in comparison with experimental data (black) [13] for: a) quasi-static lap shear test; b) quasi-static KS-2-0° test; c) quasi-static T joint*

To show the influence of the specimen stiffness, more precise the resistance of the specimen to buckling in the surrounding area of the rivet, on the loading capacity, shear specimens with stiffnesses

© 2015 Copyright by DYNAmore GmbH

between the standard lap shear specimen (low specimen stiffness) and the KS-2-0° specimen (high specimen stiffness) are simulated with a detailed model. Four variations of the lap shear specimen are chosen, which are shown in Fig. 8. Two with an increased overlap (125% - 125ue; 200% - 200ue), one with an increased width (200% - 200b) and one specimen were both, overlap and width, are increased by 200% (200ue_200b). In all cases the measuring length and the clamping length are taken from [14].

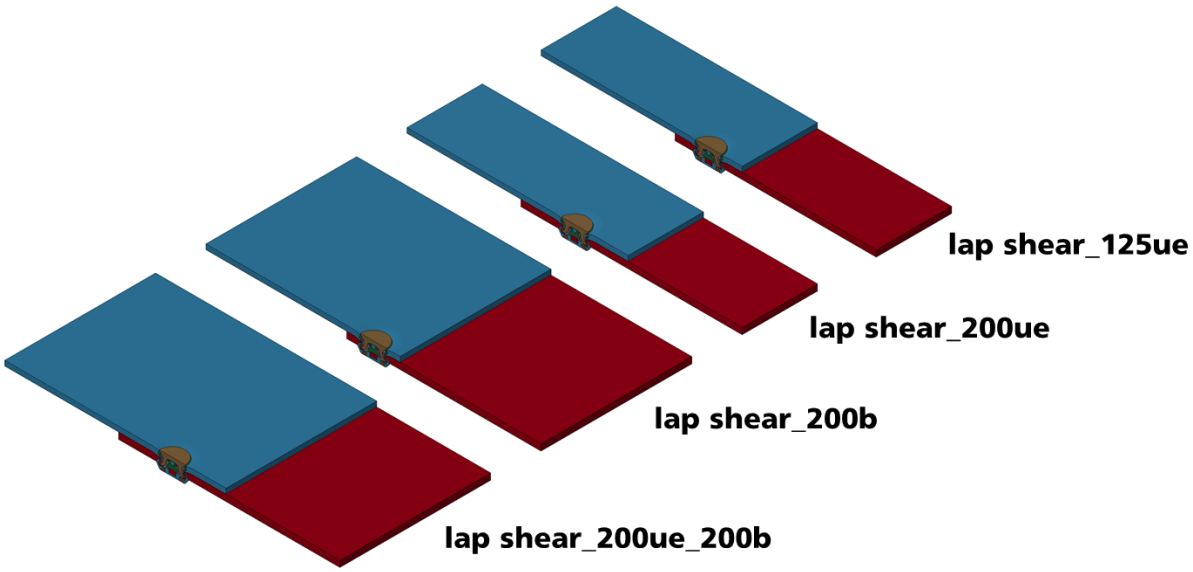

Fig.8: Geometry of the four variations of the lap shear specimen

The simulation results are shown in Fig. 9. Increasing the overlap leads to an increasing maximum force, but still with the highest chosen overlap (200ue) the maximum force is lower than in case of the KS-2-0° specimen. The variation of the width alone doesn't affect the maximum force, but combined with a higher overlap (200ue_200b) the simulation result is similar to the KS-2-0° specimen. Hence it is possible to generate specimens with various stiffnesses as well as maximum load capacities in the range between the KS-2-0° and the lap shear specimen.

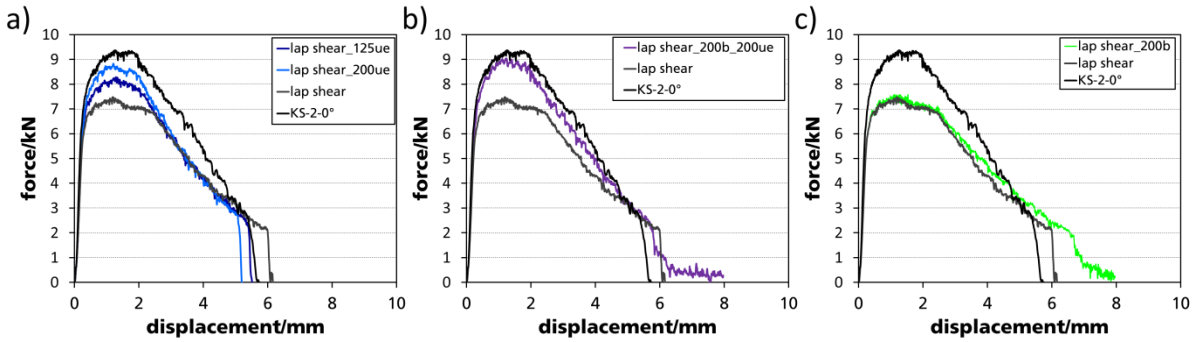

Fig.9: Global force vs. displacement curves for lap shear specimen as a result of simulations with the detailed model and variation of: a) overlap; b) width; c) overlap and width

A proper simplified model for self-piercing riveted joints should be able to describe the presented behavior depending on the specimen stiffness. Because this behavior is primarily caused by the weakening of the sheets in the area of the joint, for a modification of the simplified model the first step is to take the hole in the sheets into account. Just modeling the hole, with the same parameters for the **`*Constrained_SPR3 (Model 2),`** improves the model quality. The loading of the sheets is shifted to the pressure side (see Fig. 6) and the deformations, more precisely the buckling, are closer to the experiment (see Fig. 10 a)). Likewise in the force displacement curve a first local maximum is reached at the time the specimen starts buckling (see Fig. 10 b)). The value of this first maximum corresponds to the maximum force reached in lap shear experiments. The value of the second maximum is equal to the force maximum in lap shear simulation without a hole. This is caused by an incorrect reaction of the simplified model to the changed sheet deformation.

© 2015 Copyright by DYNAmore GmbH

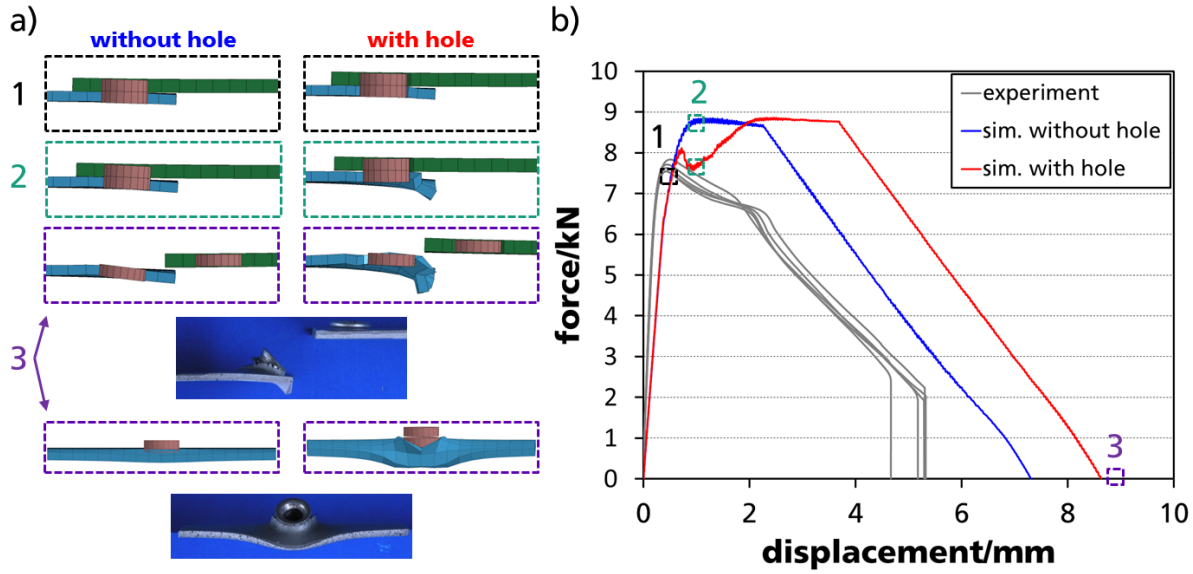

Fig.10: a) Deformation in the area of the rivet during lap shear simulation with and without hole in the sheets compared with experimental results (Simulation with shell elements, shell thickness used for illustration); b) Global force vs. displacement curves for lap shear specimen as a result of simulations with and without hole in the sheets using the ****Constrained_SPR3 (Model 2)*** *– KS-2-0° specimen used for parameter identification*

The future topic in the field of modeling self-piercing riveted joints is to identify parameters, which are characteristic of the influence of the specimen stiffness to the shear load capacity. Based on these parameters and the modeling of the hole pierced by the rivet, the ***Constrained_SPR3** could be modified, so that changes in the maximum force can be represented. This is one of the working packages in the ongoing German research project called "Characterization and modeling of mechanical joints with one-sided accessibility for profile intensive lightweight construction under crash loading".

6 Summary

In these investigations, the ***Constrained_SPR3 (Model 2)** is used as a simplified model for self-piercing riveted joints.
First a short model description is given and a proper way for the identification of the model parameters is shown. Using appropriate model parameters the ***Constrained_SPR3 (Model 2)** shows good results in case of simulation of KS-2 specimens as well as more complex specimens like the T joint. This leads to the conclusion that the ***Constrained_SPR3 (Model 2)** is a suitable model for self-piercing riveted joints.
Secondly a weakness of the actual modeling technique in case of shear load is shown. A dependence of the shear load capacity on the specimen stiffness could be observed in simulations with a detailed model. This dependence is not captured by the simplified models. Modeling of undamaged sheets could be identified as reason for the discrepancies. For further improvement of the quality of simplified models, it is necessary to model a hole in the sheets in the area of the rivet.

7 Acknowledgments

The Industrial Collective Research project (IGF-Nr. 18289 N / FOSTA P1032) of the Research Association for Steel Application (FOSTA), Sohnstrasse 65, 40237 Duesseldorf has been funded by the German Federation of Industrial Research Associations „Otto von Guericke" e.V. (AiF) within the program for sponsorship of Industrial Collective Research (IGF) of the German Federal Ministry of Economic Affairs and Energy (BMWi) based on an enactment of the German Bundestag.

The authors would like to thank all parties involved for the funding and the support. Sincere thanks are also given to all cooperating companies and their representatives for the excellent cooperation during the project.

© 2015 Copyright by DYNAmore GmbH

8 Literature

[1] He, X., Pearson, I.,Young, K.: ”Self-pierce riveting for sheet materials: State of the art”, Journal of Materials Processing Technology, Volume 199, Issues 1–3, 2008, Pages 27-36

[2] DIN 8593-5:2003-09: “Fertigungsverfahren Fügen; Teil 5: Fügen durch Umformen; Einordnung, Unterteilung, Begriffe”, 2003

[3] Seeger, F., Feucht, M., Frank, Th., Keding, B., Haufe, A.: “An Investigation on Spot Weld Modelling for Crash Simulation with LS-DYNA”, 4th LS-DYNA Anwenderforum, 2005

[4] Bier, M., Liebold, C., Haufe, A., Klamser, H.: “Evaluation of a Rate-Dependent, Elasto-Plastic Cohesive Zone Mixed-Mode Consitutive Model for Spot Weld Modeling”, 9th LS-DYNA Anwenderforum, 2010

[5] Marzi, S., Hesebeck, O., Brede, M., Kleiner, F.: “A rate dependet elastoplastic cohseive zone mixed mode model for crash analysis of adhesivly bondes joints”, 7th European LS-DYNA Conference, 2009

[6] Hanssen, A.G., Olovsson, L., Porcaro, R., Langseth, M.: ”A large-scale finite element point-connector model for self-piercing rivet connections”, European Journal of Mechanics - A/Solids, Volume 29, Issue 4, 2010, Pages 484-495

[7] LS-DYNA Keyword Users’s Manual, Version 971 R6.0.0, Livermore Software Technology Corporation (LSTC), 2012

[8] Sommer, S., Maier, J.: “Failure Modeling of a self-piercing riveted joint using LS-Dyna”, 8th European LS-DYNA Conference, 2011

[9] Bier, M., Sommer, S.: “Advanced investigations on a simplified modeling method of self-piercing riveted joints for crash simulation”, 11th LS-DYNA Anwenderforum, 2012

[10] Buckley, M., Lucas, S., Sturt, R.: “A new material model for self piercing rivet joints in full vehicle crash test simulations; *MAT_SPR_JLR”, 9th European LS-DYNA Conference, 2013

[11] Buckley, M., Lucas, S., Sturt, R.: “Modeling self-piercing riveted joint failures in automotive crash structures”, 10th International LS-DYNA Users Conference, 2008

[12] Bier, M., Sommer, S.: “Simplified modeling of self-piercing riveted joints for crash simulation with a modified version of *CONSTRAINED_INTERPOLATION_SPOTWELD”, 9th European LS-DYNA Conference, 2013

[13] Forschungsvereinigung Stahlanwendung e.V. FOSTA: “Experimentelle Untersuchung und Simulation des Crashverhaltens mechanisch gefügter Verbindungen (P 837 / IGF-Nr. 352 ZBG)”, Düsseldorf, 2013, to be published

[14] Stahl-Eisen-Prüfblatt (SEP) 1231: „Determination of Mechanical Properties on Joined Sheet Metals by High-Speed Tensile Testing“, 1st Edtion, 08.2013

© 2015 Copyright by DYNAmore GmbH